ACS APPLIED MATERIALS & INTERFACES

Research Article

www.acsami.org

Atmospheric-Pressure Plasma-Enhanced Chemical Vapor Deposition of a-SiCN:H Films: Role of Precursors on the Film Growth and Properties

Srinivasan Guruvenket,*[,†] Steven Andrie,[‡] Mark Simon,[‡] Kyle W. Johnson,[‡] and Robert A. Sailer[†]

[†]Center for Nanoscale Science and Engineering, North Dakota State University, Research Park Drive, Fargo, North Dakota 58102, United States

[‡]Department of Mechanical Engineering, North Dakota State University, 111 Dolve Hall, Fargo, North Dakota 58102, United States

Supporting Information

ABSTRACT: Atmospheric pressure plasma enhanced chemical vapor deposition (AP-PECVD) using Surfx Atomflow™ 250D APPJ was utilized to synthesize amorphous silicon carbonitride coatings using tetramethyldisilizane (TMDZ) and hexamethyldisilizane (HMDZ) as the single source precursors. The effect of precursor chemistry and substrate temperature (T_s) on the properties of a-SiCN:H films were evaluated, while nitrogen was used as the reactive gas. Surface morphology of the films was evaluated using atomic force microscopy (AFM); chemical properties were determined using Fourier transform infrared spectroscopy (FTIR); thickness and optical properties were determined using spectroscopic ellipsometry and mechanical properties were determined using nanoindentation. In general, films deposited at substrate temperature (T_s) < 200 °C contained organic moieties, while the films deposited at T_s > 200 °C depicted strong Si−N and Si-CN absorption. Refractive indices (n) of the thin films showed values between 1.5 and 2.0, depending on the deposition parameters. Mechanical properties of the films determined using nanoindentation revealed that these films have hardness between 0.5 GPa and 15 GPa, depending on the T_s value. AFM evaluation of the films showed high roughness (R_a) values of 2−3 nm for the films grown at low T_s (<250 °C) while the films grown at $T_s \geq$ 300 °C exhibited atomically smooth surface with R_a of ∼0.5 nm. Based on the gas-phase (plasma) chemistry, precursor chemistry and the other experimental observations, a possible growth model that prevails in the AP-PECVD of a-SiCN:H thin films is proposed.

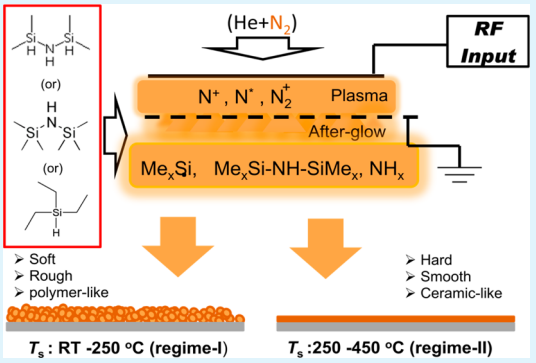

KEYWORDS: *atmospheric pressure plasma, antireflective coatings, thin film growth model, tetramethyldisilizane (TMDZ), hexamethyldisilizane (HMDZ) and triethylsilane (TES)*

1. INTRODUCTION

Plasma processing routes are commonly used to modify the surface properties of polymers and to deposit thin films to obtain desired surface properties.[1−3] While vacuum-based plasma processes are well-studied, atmospheric pressure plasma (APP) processes are comparatively less explored. APP routes have shown promising results in surface functionalization and plasma polymerization to get desired surface properties, such as hydrophobic/phillic, antimicrobial, etc.[4−7] Recently, there has been a growing interest in utilizing APP routes to deposit functional thin films that have potential in applications such as antireflective coatings for solar cells, dielectric layers in microelectronic devices, biomedical applications, and surface protective layers, (such as corrosion resistance, moisture barriers, etc.).[8−10] Earlier, we reported the use of AP-PECVD processing to form transparent conducting oxide coatings such as tin oxide (SnO_x), indium-doped tin oxide (In:SnO_x, (ITO)), zinc oxide (ZnO), and aluminum-doped zinc oxide (Al:ZnO) coatings.[11−13] Bardos et al. summarized atmospheric-pressure plasma-enhanced chemical vapor deposition (AP-PECVD) synthesized thin films of metal oxides, plasma polymers, and diamond-like carbon (DLC) materials, which clearly shows the growing interest in the use of the AP-PECVD process for functional coating deposition.[14]

a-SiN_x:H thin films deposited via PECVD using silane and nitrogen−hydrogen/ammonia mixtures or by reactive sputtering are commonly used as antireflection coatings in c-Si solar cells.[15,16] Given the hazards involved in handling silane gases, as an alternate, Kang et al. demonstrated the deposition of a-SiCN:H thin films using PECVD with a single-source solid precursor.[17] In an similar effort, Wrobel et al. investigated the role of metal−organic single source precursors and the reactive gas chemistries on the growth of a-SiC:H and a-SiCN:H films, using a vacuum-based remote PECVD process.[18−20] Hopfe et al., using a linear extended arc plasma source with silane and nitrogen/ammonia, deposited a-SiN_x:H at atmospheric pres-

Received: July 6, 2012
Accepted: September 14, 2012
Published: September 14, 2012

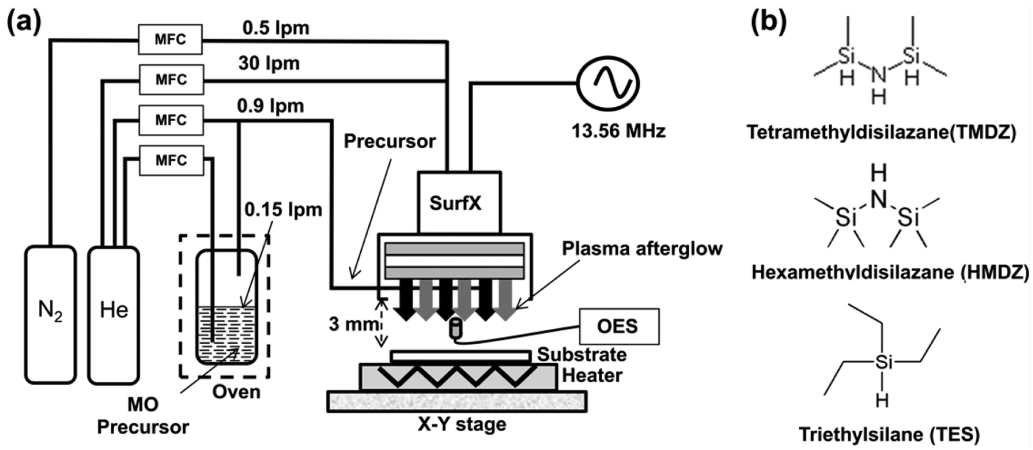

Figure 1. (a) Schematic representation of the AP-PECVD setup used for the synthesis of a-SiCN:H thin films and (b) chemical structure of the metal−organic precursors.

sure.[21] Enabling the use of atmospheric pressure processes that utilize nontoxic precursors will add benefits in terms of production and equipment maintenance costs. To this end, recently we demonstrated the deposition of a-SiCN:H thin films using triethlysilane ($HSiEt_3$, TES) as the precursor using the Surfx Atmoflow 200 source.[22] The interaction between the precursor and the active nitrogen species in the afterglow region of the plasma and on the substrate were deemed responsible for the observed film properties. Interestingly, films rich in Si−N bonds were obtained from a precursor that did not have nitrogen in it, which showed that the activated nitrogen species from the plasma (reactive gas) has been incorporated into the growing film to form Si−N and Si−C−N bonds.

In this investigation, we evaluate the effect of precursor chemistries on the properties of a-SiCN:H films, where tetramethyldisilzane (TMDZ) consisting of Si−N, Si−H, Si−C, and N−H bonds and hexamethyldisilazane (HMDZ), consisting of Si−N, Si−C and N−H bond, are considered as precursors for a-SiCN:H thin film deposition. The properties of a-SiCN:H films are compared with results previously obtained using TES as a precursor that consisted of Si−H and Si−C bonds alone. The fundamental processes governing the film growth via AP-PECVD will be discussed in detail on the basis of the observed thin film's properties and the plasma characteristics.

2. EXPERIMENTAL PROCEDURE

2.1. Deposition of a-SiCN:H Coatings. Thin films of a-SiCN:H were deposited using a Surfx Atomflow250D APPJ system that is described in detail elsewhere.[11,22,23] A schematic description of the AP-PECVD process and gas flow is presented in Figure1a. TMDZ and HMDZ were used as the precursors (liquid at room temperature and ambient pressure) with vapor pressures (P_v) of 25 and 22.9 mmHg at 20 °C, respectively. The chemical structure of the TMDZ, HMDZ, and TES are shown in Figure 1b. The precursors were obtained from Gelest, USA and were used as-received. Precursors were delivered to the plasma source from a heated bubbler. In order to compare the effect of precursors on the deposition rate of the a-SiCN:H thin films, the precursor bubblers were heated to various temperatures to maintain a constant vapor pressure. The temperature was determined to be 30 ± 1 °C and 36 ± 1 °C for TMDZ and HMDZ, respectively, using the Clausius−Clapeyron equation. The aforementioned temperatures were maintained to obtain a vapor pressure of ∼45 mmHg (similar to the condition maintained in our previous work with TES[22]). In order to prevent precursor condensation, the delivery lines were maintained at 100 °C and the plasma head was held at 125 °C. Helium and nitrogen (N_2) were used as the plasma and reactive gases, respectively, and their flows were maintained at 30 and 0.5 lpm, respectively, while the precursor carrier gas (He), which passes through the bubbler, was kept at a flowrate of 0.15 lpm. In this investigation, plasma power was held a constant at 140 ± 10 W, while the substrate temperature (T_s) was varied from room temperature (RT, 25 °C) to 450 °C with ±10 °C accuracy. The substrate-to-plasma distance was fixed at 3 mm. Crystalline double-side-polished intrinsic silicon (i-Si) wafers (2.5 cm × 2.5 cm), cleaned with isopropyl alcohol, were used as the substrates. Depositions were carried out by moving the heated substrate holder (platen) under the plasma source in a serpentine motion. The serpentine motion parameters (length, width, step size, and velocity) were chosen to produce uniform film deposition across the entire substrate surface. In order to preclude oxygen contamination, the plasma source was located inside an inert atmosphere (nitrogen-filled glovebox).

2.2. Plasma and Thin Film Characterization. To investigate the chemical (bonding) structure of the films, Fourier transform infrared (FTIR) spectroscopy was performed using a Thermo Scientific Nicolet 8700 instrument, spectra were collected between 400 cm^{-1} to 4000 cm^{-1} with a 2 cm^{-1} resolution, and to improve the signal-to-noise ratio, 64 scans were performed. Surface morphology and the quantitative details on the surface roughness of the films were obtained using atomic force microscopy (AFM) (Veeco DI-3100). Optical constants and thickness of the films were determined using a J.A. Woollam VASE spectroscopic ellipsometer with modeling and data analyses realized using the WVASE software package. Ellipsometric Ψ and Δ data were acquired at three angles of incidence (60°, 67°, and 74°) over the spectral range of 300−780 nm, in steps of 10 nm. Optical constants and thickness of the films was determined by modeling a Cauchy/silicon nitride film on a c-Si substrate.

Density (ρ) of the deposited a-SiCN:H films were determined using a gravimetric method. The i-Si wafers (1 in. × 1 in.) were weighed before and after the deposition, using a Sartorins-CP2P balance (with an accuracy of 0.002 mg). The film thickness, as determined by spectroscopic ellipsometry measurements, and the surface area of the sample, determined using a OGP Smartscope (1 μm accuracy), were used to calculate the density. The hardness (H) and reduced Young's modulus (E_r) of the coatings were determined by depth-sensitive indentation, using a triboindenter system (Hysitron, Inc.) equipped with a Berkovich pyramidal tip. The applied loads ranged between 1 and 5 mN. For each sample, H and E_r were obtained from the average of 20 indentations using the method proposed by Oliver and Pharr.[24] Care has been taken in selecting the maximum load to ensure that the measurements were performed at conditions within 10% of the film thickness, to minimize substrate effects.

Optical emission spectroscopy (OES) analyses were performed using an Ocean Optics SD 2000 spectrophotometer coupled with an optical fiber to characterize the afterglow region of the Surfx 250 D

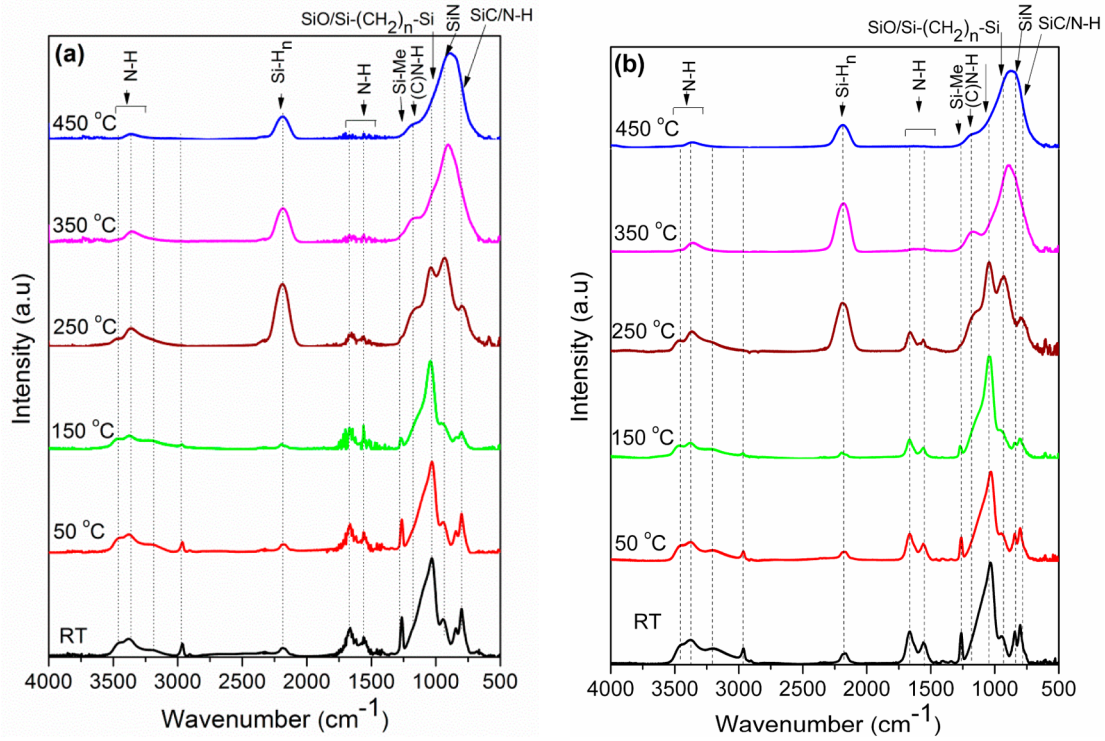

Figure 2. FTIR spectra of AP-PECVD-derived a-SiCN:H thin films from (a) tetramethyldisilizane (TMDZ) and (b) hexamethyldisilizane (HMDZ).

plasma source, as illustrated in Figure 1. The optical fiber was placed close to the lower electrode to collect the light intensity normal to the electrode. OES spectra were measured over a range of 180−890 nm, with a resolution of 0.4 nm.

3. RESULTS AND DISCUSSION

The role of T_s and the precursor chemistry on the growth and the properties of the a-SiCN:H films are studied. Films of a-SiCN:H were deposited with TMDZ and HMDZ at T_s from RT to 450 °C, while all other deposition parameters were held constant. Figures 2a and 2b depict the FTIR spectra of the a-SiCN:H films deposited using TMDZ and HMDZ, respectively. a-SiCN:H films deposited using a TMDZ precursor at RT, 50, and 150 °C exhibit prominent features corresponding to Si−Me, Si−$(CH_2)_n$−Si/SiO and SiC at 1263, 1030, and 800 cm^{-1}, respectively. Features corresponding to Si−NH_2/Si−CH, C−H_n, Si−OH/Si−NH_2/Si−NH−Si, Si−H_n and Si−NH−Si can be observed at 1500−1700, 2900−2960, 3200−3500, 2180, and 937 cm^{-1}, respectively.[2,22,25,26] With T_s increasing to ≥ 250 °C, significant changes in the absorption features were noticed. In addition to the Si−$(CH_2)_n$−Si peak (at 1030−1050 cm^{-1}), a peak at ∼930 cm^{-1} corresponding to Si−NH/Si−N, can be observed (for films deposited at 250 °C); with further increases in T_s, increases in absorption corresponding to Si−N vibration can be noticed with a concurrent decrease in Si−$(CH_2)_n$−Si absorption.[27] No characteristic peak of Si−$(CH_2)_n$−Si could be observed for the films deposited at 450 °C, while corresponding Si−Me (at 1263 cm^{-1}) and N−H absorptions become insignificant. It is also interesting to note that the vibration corresponding to Si−H_n and/or Si-NH_2 at 2150−2200 cm^{-1} becomes significant at 250 °C and decreases with further increases in T_s.[27]

Similar FTIR spectral features, as a function of T_s, were found for the a-SiCN:H films that were deposited with HMDZ (refer to Figure 2b). The chemical characteristic features were analogous to our earlier observations made for a-SiCN:H films deposited with TES at similar conditions.[22] Based on these observations, at lower T_s (<250 °C), the films exhibit strong organic-like features (denoted by the presence of Si−CH_3 groups), while with increasing T_s (≥250 °C), films exhibit ceramic-like features (Si−C, Si−N, and SiCN bonds). These observations depict a temperature-assisted growth occurring on the substrate surface, where at lower T_s the adatoms/molecules have low energy for thermal decomposition, surface diffusion, and chemical reaction, leading to the formation of organic-like films. With increasing T_s, chemical desorption, thermally induced reaction, and surface diffusion occur more rapidly, leading to the formation of ceramic-like a-SiCN:H films. It is interesting to note that we observe film formation with HMDZ using an atmospheric-pressure remote PECVD process with nitrogen reactive radicals. Earlier, Wrobel et al. showed no films with HMDZ (as precursor) and N_2, H_2, or N_2−H_2 (as the reactive gases), utilizing a microwave-based vacuum remote PECVD reactor, and attributed it to the absence of Si−H bond in HMDZ.[28]

Surface topography/morphology of the a-SiCN:H films were assessed using AFM. Figures 3a and 3b depict the surface morphology of the films deposited with TMDZ and HMDZ, respectively, at RT and 450 °C, while Figure 3c depicts change in the average roughness (R_a) as the function of T_s for the a-SiCN:H films deposited with TMDZ and HMDZ. The change in R_a with T_s for the films deposited with TES is also provided in Figure 3c for comparison. a-SiCN:H films deposited using TMDZ at RT exhibit an R_a value of ∼26 nm, which decreased as T_s increased and a minimal value of R_a = 0.8 nm obtained at 450 °C. a-SiCN:H films deposited using HMDZ depicted a similar trend; however, a lower R_a value of 12.4 nm was observed for films deposited at RT. Earlier, using TES under similar deposition conditions, a similar trend in the film roughness R_a with T_s was observed (shown in Figure 3c).[22]

dx.doi.org/10.1021/am301157p | ACS Appl. Mater. Interfaces 2012, 4, 5293−5299

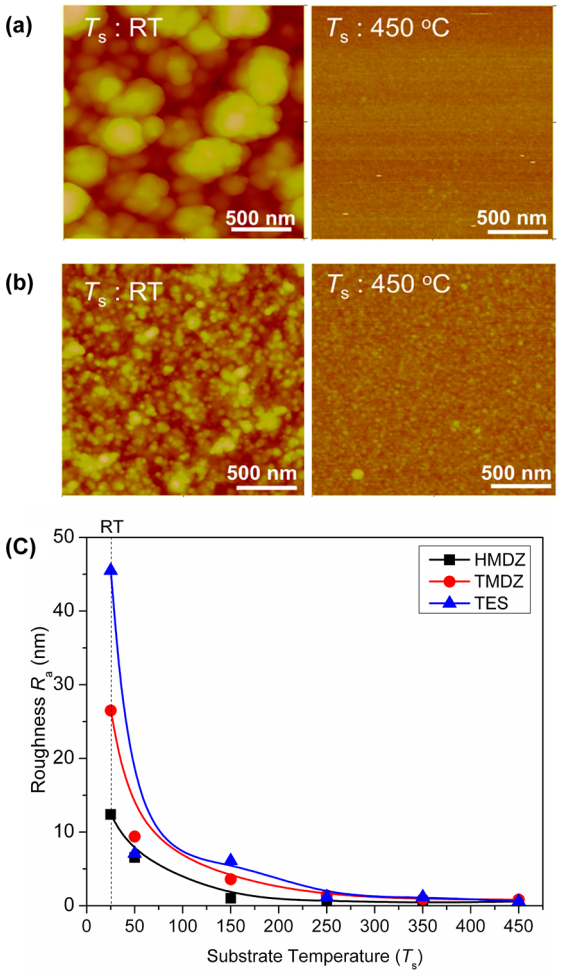

Figure 3. AFM morphology of a-SiCN:H films (a) at RT and 450 °C using TMDZ and (b) at RT and 450 °C using HMDZ; (c) change in roughness with substrate temperature (T_s) for films deposited with TMDZ, HMDZ, and TES.[22]

Generally, a decrease in R_a with increasing T_s depicts temperature-induced surface diffusion of the ad-atoms/molecules and increased chemical reactivity between the adsorbed species and/or with the plasma reactive radicals. The R_a values observed for a-SiCN:H films deposited using TMDZ, HMDZ, and TES are comparable to the R_a values obtained for a-SiN_x and a-SiCN:H films obtained using vacuum-based PVD, CVD, and PECVD processes.[16,29]

Optical constants (n and k) of a-SiCN:H coatings were determined using spectroscopic ellipsometry, and the determined values, as a function of T_s, are plotted in Figure 4a. Generally as T_s increases in the values of n and ρ can be observed. a-SiCN:H films deposited at 450 °C with TMDZ and HMDZ depict n of 1.98 and 1.93, respectively. The change in n values for a-SiCN:H films synthesized using TES is shown for comparison, and at 450 °C, we observe a n value of 1.9. The higher n values observed for the films deposited with TMDZ and HMDZ can be attributed to the presence of nitrogen atoms in the parent precursor molecule in TMDZ and HMDZ. Similar n values were reported for a-SiN_x:H and a-SiCN:H films, which are suitable for antireflective coating applications in c-Si solar cells.[16,17,30]

Figure 4b depicts the change in density (ρ) of the film as the function of T_s. As T_s increases, an increase in ρ can be observed.

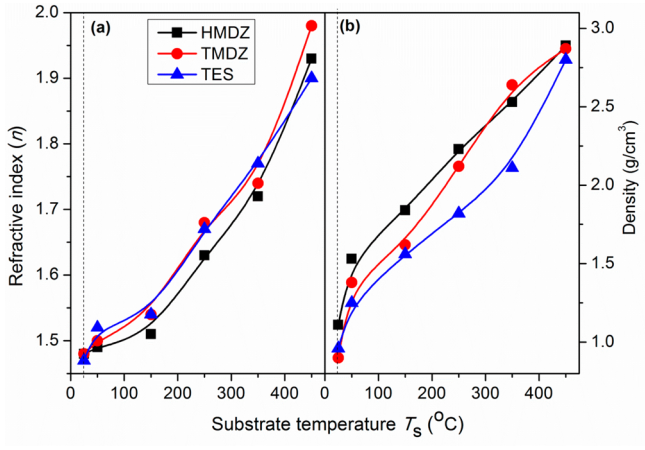

Figure 4. Change in (a) refractive index (n) and (b) density (ρ) of a-SiCH:N deposited using TMDS, HMDS, and TES, as a function of the substrate temperature (T_s).

a-SiCN:H films deposited using TMDZ and HMDZ at RT exhibits ρ values of 0.9 and 1.1 g/cm^3, respectively, while the films deposited at 450 °C have ρ of 2.87 and 2.89 g/cm^3, respectively. a-SiCN:H films deposited from TES showed ρ of 0.9 and 2.8 g/cm^3 at RT and 450 °C, respectively. This increase in ρ with increase in T_S exhibits the transformation from polymer-like porous film to ceramic-like dense film. The ρ values observed for a-SiCN:H films are comparable with those for a-SiCN:H (3.0 g/cm^3) and a-SiN_x (2.8 g/cm^3) films deposited using a vacuum PECVD process, while the bulk densities of 3.18 and 3.21 g/cm^3 are reported for bulk Si_3N_4 and SiC, respectively.[18,31,32]

Mechanical properties of a-SiCN:H films were evaluated using nanoindentation; the measured H and E_r values, each as a function of T_S, are depicted in Figure 5. With increasing T_s, an

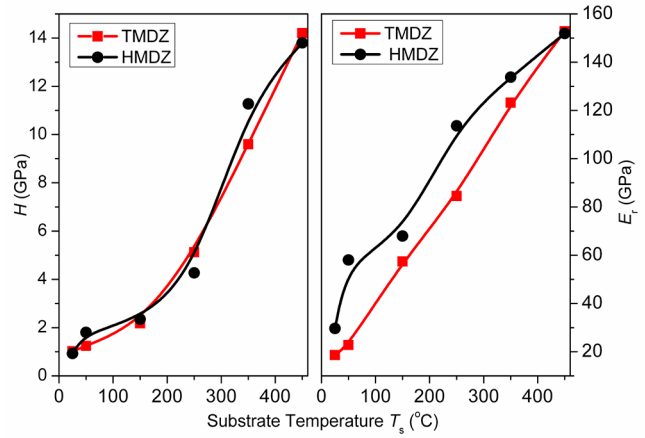

Figure 5. Hardness (H) and reduced Young's modulus (E_r) of a-SiCH:N deposited using (a) TMDS and (b) HMDS.

increase in the H and E_r values for TMDZ and HMDZ can be observed. The films deposited using TMDZ at RT depict a value of H = 1.0 GPa, which gradually increases and reaches a maximum value of 14.2 GPa at T_s = 450 °C. Similar observations were made for the films deposited with HMDS, where a maximum H value of 13.8 GPa was observed for films deposited at T_s = 450 °C. An increase in E_r value, as a function of T_s, was observed for the a-SiCN:H films deposited using

dx.doi.org/10.1021/am301157p | ACS Appl. Mater. Interfaces 2012, 4, 5293−5299

TMDZ and HMDZ. a-SiCN:H films obtained using HMDZ show a higher E_r value (151.9 GPa) than that of TMDS (142.1 GPa). The H and E_r values obtained with an AP-PECVD process using TES, TMDZ, and HMDZ are comparable with the values that were previous reported for vacuum-based thin film processes such as CVD and PECVD.[2,27]

In addition, the increase in H and E_r values with increasing T_s shows the change in the structure, chemical composition and density of the a-SiCN:H thin films. a-SiCN:H films deposited at lower T_s are soft, porous, and exhibit the presence of organic groups (Si−$(CH_3)_n$) (as observed from the FTIR analysis), while the a-SiCN:H that was deposited at higher T_s forms hard, dense films consisting of SiC, SiN, and SiCN bonds.

In order to understand the effect of the precursors on the growth mechanism of the thin films obtained using AP-PECVD, the deposition rates of the a-SiCN:H films were analyzed. Figure 6a depicts the deposition rate of a-SiCN:H

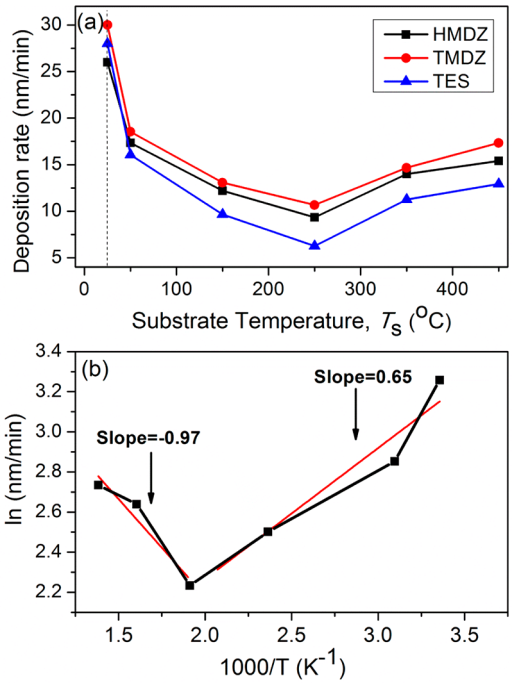

Figure 6. (a) Deposition rate versus T_s and (b) deposition rate, as function of 1000/T_s (K^{-1}).

films, as a function of T_s. a-SiCN:H films deposited from TMDZ at RT showed a thickness of 450 nm, which decreased with increasing T_s; this trend continued until T_s reached 250 °C, where a film thickness of 160 nm was observed. Above a T_s value of 250 °C, the thickness increased as T_s increased; at 450 °C, a film thickness of 260 nm was observed. Similar trends were observed for a-SiCN:H films deposited with HMDZ. The growth rate of a-SiCN:H films obtained from TES is also provided for reference. The deposition rate, as a function of 1000/T_s for a-SiCN:H films using HMDZ, is depicted in Figure 6b, which exhibits positive and negative slopes between 25 to 250 °C (region I) and 250 to 425 °C (region II), respectively.

Negative activation energy (positive slope (region I)) can be attributed to desorption of the organic moieties (CH_n) from the adsorbed species on the substrate, and the improved surface diffusion of the adsorbed species on the substrate can be attributed to the thermal activation. Casserly et al. investigated the effect of T_s on plasma-polymerized PMMA films, where they observed a decrease in film thickness with an increase in T_s (~40−145 °C).[33] They attribute the decrease in the film thickness to the increases in desorption of the species from the substrate surface. We observe a decrease in the film thickness with a concurrent decrease in the roughness, as a function of T_s in a-SiCN:H thin films, which indicates a thermally induced surface hopping and diffusion of the adsorbed species that occur with increases in T_s, leading to the formation of smoother films. The increases in density (ρ), hardness (H), and refractive index (n) with increases in T_s support the aforementioned observation.

In region II, the positive activation energy (a negative slope) can be attributed to a thermally driven chemical reaction similar to classical chemical vapor deposition (CVD). In a CVD process, the growth rate of a film depends on the gas-phase diffusion, reaction rate, mass-transfer coefficient (boundary layer thickness), and the surface diffusion/jumping frequency of the adsorbed species. These aforementioned processes strongly depend on geometry of the reactor, pressure and substrate temperature. Gas-phase diffusion of the radicals depends on the pressure and temperature, according to the relation $\sim T_s^{3/2}/P$,[34] where P is the pressure. In this study, since pressure was maintained constant during the deposition, an increase in T_s will favor gas-phase diffusion of the precursor molecules/radicals toward the substrate. Also, the surface reaction rate increases with T_s, in accordance with Arrhenius behavior, which can be explained by the relation $k_s = [\exp(-E/RT_s)]$, where E is the activation energy and R is the gas constant.[35] At low T_s, the reaction rate controls the film growth (i.e., surface-reaction-controlled growth); on the other hand, at high T_s, mass transfer (h_g) controls film growth. In addition, with increasing T_s, higher displacement of the adsorbed species on the surface occurs, with a concurrent decrease in surface energy, both supporting better surface diffusion, thus leading to smoother films.[34]

In the case of the a-SiCN:H films obtained at T_s > 250 °C via AP-PECVD, the increase in film thickness, with a concurrent decrease in R_a, resulted in an increase in H and ρ, and a change in chemical features (from FTIR); all of these observations are indicative of an enhanced reaction between the adsorbed species at higher temperatures. Therefore, the enhanced reactivity and better radical diffusion can beaccountable for the increase in film thickness at T_s, ranging from 250 °C to 450 °C. The combination of thermally induced desorption of organic moieties, improved chemical reactions between the adsorbed species with the growing film, and the higher adatom mobility leads to the formation of dense, ceramic-like films. Experimental observations such as increases in Si−N and decreases in Si−Me (from FTIR), decreases in R_a, and increases in n, ρ, H, and E_r, each as a function of T_s, support the aforementioned statements.

Among the two precursors investigated in this study and the results obtained from our previous study using TES, a-SiCN:H films obtained from TMDZ display the highest deposition rates. The chemical structure of TMDZ consists of two Si−H bonds, while TES and HMDZ have one and no Si−H bonds in their molecular structures, respectively. The higher deposition rate can be attributed to the presence of additional Si−H and N−H bonds in the structure of the TMDZ precursor molecule. Using a vacuum remote plasma technique, Wrobel et al. demonstrated that TMDZ has better ability to form a-SiC:H films, because of the presence of the Si−H bond in the parent precursor molecule.[27] From their observations, Si−H bonds present in precursor molecules are held responsible for the film formation

via chemical reactions between the plasma-activated nitrogen and/or hydrogen to form Si−N and Si-CN bonds in the films. In vacuum remote plasma, HMDZ, which has no Si−H bonds, did not undergo any chemical reaction to form Si-based thin films and is considered as a non-film-forming precursor. However, in the present investigation, we observed that HMDZ is a film-forming precursor. This could be due to the unique nature of the remote plasma setup used by the authors; however, HMDZ has been used as a source for a-SiCN:H thin films, using direct and remote PECVD at low pressures, by several other authors.[36,37]

OES spectra of a He+N_2 plasma is shown in Figure 7; the figure shows that the afterglow region of the plasma consists of

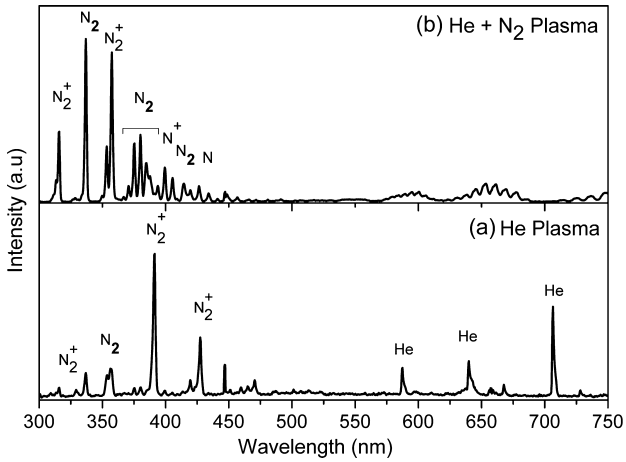

Figure 7. OES spectra (a) He and (b) He+N_2 plasma at 120 W of plasma power (from ref 22).

N^+, $N^•$, and N_2^+ species formed by electron impact ionization, dissociation, and penning ionization, respectively (with excited He).[28] The activated nitrogen species in the afterglow region can react with the precursor molecules and, hence, activate them in several ways. The activated precursor molecule and the nitrogen radicals can undergo reaction in the gas phase and also on the substrate surface in several ways; based on the experimental observations (from the thin film analysis, OES), potential chemical reactions that would lead to the formation of a-SiCN:H thin films are discussed below.

The TMDZ precursor molecule injected in the afterglow region can be disassociated by the $N^•$, radical as shown below:

$$2\dot{N} + Me_2SiHNHSiHMe_2 \rightarrow 2[\dot{Me_2}Si] + 2NH + H \quad (1)$$

The above reaction may take several steps to form the products depicted above, but it will form these thermodynamically stable species. N^+ and N_2^+ species can also initiate the reaction to form the silyl radical shown above.

Si−H bonds present in the TMDZ precursor molecule are considered responsible for precursor fragmentation in the afterglow region; the absence of a Si−H bond in HMDZ was attributed to the non-film-forming properties; however, in our investigation, we observe a-SiCN:H film formation with HMDS.[28] The possible initiation reaction that could occur between HMDS and afterglow region is

$$\dot{N} + Me_3SiNHSiMe_3 \rightarrow 2[\dot{Me_3}Si] + NH + N \quad (2)$$

As stated earlier, these reactions can occur in multiple steps and can be initiated by N^+ and N_2^+ species.

The $\dot{Me_x}Si$ (x = 2 or 3) and NH radicals readily recombine on the hot substrate as follows:

$$\dot{Me_x}Si + NH \rightarrow [Me_xSiNH] \quad (3)$$

$$[Me_xSiNH] + \dot{Me_x}Si \rightarrow Me_xSi{-}N(H){-}SiMe_x \quad (4)$$

Formation of Me_2SiHN and $Me_2SiNHSiMe_2$ from TMDZ via reaction with activated nitrogen species in a RP-CVD process was reported earlier.[28] FTIR spectra (Figures 2a and 2b) for the a-SiCN:H films exhibit the formation of NH_n bonds (at 3200−3500 cm^{-1}) and (Si−(CH_2)−Si) and Si−Me_x group (1030 and 1263 cm^{-1}) for the films that are deposited at lower T_s (<250 °C), supporting the possible occurrence of the above chemical reactions.

Upon reaching the substrate, $Me_xSi{-}N(H){-}SiMe_x$ species decompose to form methylsilanimine ($Me_xSi{=}NH$) and methylsililene ($Me_xSi{:}$),[28] as shown below:

$$\dot{Me_x}SiHNHSiMe_x \xrightarrow{\Delta} Me_xSi = NH + Me_xSiH\cdot \quad (5)$$

$$\dot{Me_x}SiNHSiMe_x \xrightarrow{\Delta} Me_xSi = NH + Me_xSiH{:} \quad (6)$$

These silamine groups are highly reactive, transient intermediates that contribute to step growth.[22,28] Interestingly, the silamine group and Si−H vibrations are significant in FTIR in the films that are deposited above 250 °C. These products mentioned in the above equations may undergo cross-linking reactions and elimination of methyl groups (by thermal decomposition) leading to the formation of Si−N and a Si−C−N network at higher T_s values, as evident from the FTIR analysis. These results are consistent with our previous observations with triethylsilane and nitrogen plasma.

Experiments were carried out without nitrogen addition the plasma at various T_s values, and no film could be observed, even at T_s = 450 °C (with any of the aforementioned precursors) depicting that the nitrogen radical formed in the plasma is responsible for the thin film deposition.

4. CONCLUSIONS

TMDS and HMDZ were used as precursors for the synthesis of a-SiCN:H films using AP-PECVD with nitrogen as the reactive gas. The presence of Si−H bonds in TMDS accounts for the higher deposition rate, compared to that of HMDS. Despite the absence of Si−H bonds, HMDS could still be activated with the AP-PECVD process to form a-SiCN:H thin films. The T_s value plays a significant role in the structural and chemical properties of a-SiCN:H thin film. Irrespective of the precursor used, in AP-PECVD, there exist two different growth regimes. In regime I, with increasing T_s, a decrease in the deposition rate occurs, similar to that for plasma polymerization reactions; whereas in regime II, the deposition rate increases with T_s, in a manner similar to that for typical CVD processes. Generally, an increase in T_s helps to eliminate the organic moieties and formation of Si−N and Si−C−N, leading to ceramic-like film formation. Film formation occurs if and only if there exists a nitrogen plasma in the deposition zone. The absence of film formation without plasma and without nitrogen (i.e., pure He plasma) depicts that the AP-PECVD process is a radical initiated reaction, where T_s play a vital role in the structure of the deposited film.

■ ASSOCIATED CONTENT

Supporting Information

This material is available free of charge via the Internet at http://pubs.acs.org.

■ AUTHOR INFORMATION

Corresponding Author

*Fax: +1 (701)-231-5306. E-mail: guruvenket.srinivasan@ndsu.edu, guruvenkat@gmail.com.

Notes

The authors declare no competing financial interest.

■ ACKNOWLEDGMENTS

This material is based on research sponsored by the Department of Energy (Grant No. DE-FG36-08GO88160). The views and conclusions contained herein are those of the authors and should not be interpreted as necessarily representing the official policies or endorsements, either expressed or implied of the Department of Energy or the U.S. Government. Help from Mr. J. Risan for his film characterizations is greatly appreciated.

■ REFERENCES

(1) Guruvenket, S.; Iyer, G. R. S.; Shestakova, L.; Morgen, P.; Larsen, N. B.; Rao, G. M. *Appl. Surf. Sci.* **2008**, *254*, 5722−5726.
(2) Guruvenket, S.; Azzi, M.; Li, D.; Szpunar, J. A.; Martinu, L.; Klemberg-Sapieha, J. E. *Surf. Coat. Technol.* **2010**, *204*, 3358−3365.
(3) Martin, P., *Introduction to Surface Engineering and Functionally Engineered Materials*: John Wiley & Sons: New York, 2011.
(4) Pappas, D. *J. Vacuum Sci. Technol. A* **2011**, *29*, 020801.
(5) Davis, R.; El-Shafei, A.; Hauser, P. *Surf. Coat. Technol.* **2011**, *205*, 4791−4797.
(6) Yaghoubi, H.; Taghavinia, N. *Appl. Surf. Sci.* **2011**, *257*, 9836−9839.
(7) Da Ponte, G.; Sardella, E.; Fanelli, F.; d'Agostino, R.; Favia, P. *Eur. Phys. J.—Appl. Phys.* **2011**, *56*, 24023.
(8) Nowling, G. R.; Babayan, S. E.; Jankovic, V.; Hicks, R. F. *Plasma Sources Sci. Technol.* **2002**, *11*, 97−103.
(9) McSporran, N.; Hitchman, M. L.; Alexandrov, S. E.; Shamlian, S. H.; Turnbull, S.; Tuema, F. *J. Phys. IV* **2002**, *12*, 17−23.
(10) von Keudell, A.; Benedikt, J. *Plasma Process Polym.* **2010**, *7*, 376−379.
(11) Sailer, R. A.; Wagner, A.; Schmit, C.; Klaverkamp, N.; Schulz, D. L. *Surf. Coat. Technol.* **2008**, *203*, 835−838.
(12) Johnson, K.; Guruvenket, S.; Jha, S.; Halverson, B.; Olson, C.; Sailer, R. A.; Pokhodnya, K.; Schulz, D. L. In *Photovoltaic Specialists Conference (PVSC), 2009 34th IEEE*, 2009; pp 001806−001810.
(13) Johnson, K. W.; Braun, C.; Anderson, K.; Halverson, B.; Pokhodnya, K.; Guruvenket, S.; Sailer, R. A.; Schulz, D. L. In *52nd Annual Technical Conference Proceedings, Society of Vacuum Coaters*, 2009; p 327.
(14) Bardos, L.; Barankova, H. *Thin Solid Films* **2010**, *518*, 6705−6713.
(15) Janssen, L.; Windgassen, H.; Batzner, D. L.; Bitnar, B.; Neuhaus, H. *Sol. Energy Mater. Sol. Cells* **2009**, *93*, 1435−1439.
(16) Guruvenket, S.; Ghatak, J.; Satyam, P. V.; Rao, G. M. *Thin Solid Films* **2005**, *478*, 256−260.
(17) Kang, M. H.; Kim, D. S.; Ebong, A.; Rounsaville, B.; Rohatgi, A.; Okoniewska, G.; Hong, J. *J. Electrochem. Soc.* **2009**, *156*, H495−H499.
(18) Wrobel, A. M.; I. Blaszczyk-Lezak, Uznanski, P.; Glebocki, B. *Chem. Vapor Depos.* **2010**, *16*, 211215.
(19) Walkiewicz-Pietrzykowska, A.; Wrobel, A. M.; Glebocki, B. *Chem. Vapor Depos.* **2009**, *15*, 47−52.
(20) Wrobel, A. M.; A. Walkiewicz-Pietrzykowska, Uznanski, P.; Glebocki, B. *Chem. Vapor Depos.* **2011**, *17*, 186190.
(21) Hopfe, V.; Rogler, D.; Maeder, G.; Dani, I.; Landes, K.; Theophile, E.; Dzulko, M.; Rohrer, C.; Reichhold, C. *Chem. Vapor Depos.* **2005**, *11*, 510−522.
(22) Guruvenket, S.; Andrie, S.; Simon, M.; Johnson, K. W.; Sailer, R. A. *Plasma Process Polym.* **2011**, *8*, 1126−1136.
(23) Moravej, M.; Hicks, R. F. *Chem. Vapor Depos.* **2005**, *11*, 469−476.
(24) Oliver, W. C.; Pharr, G. M. *J. Mater. Res.* **1992**, *7*, 1564−1583.
(25) Awad, Y.; El Khakani, M. A.; Aktik, C.; Mouine, J.; Camire, N.; Lessard, M.; Scarlete, M.; Al-Abadleh, H. A.; Smirani, R. *Surf. Coat. Technol.* **2009**, *204*, 539−545.
(26) Di Mundo, R.; Ricci, M.; d'Agostino, R.; Fracassi, F.; Palumbo, F. *Plasma Process Polym.* **2007**, *4*, S21−S26.
(27) Wrobel, A. M.; Walkiewicz-Pietrzykowska, A.; Ahola, M.; Vayrynen, I. J.; Ferrer-Fernandez, F. J.; Gonzalez-Elipe, A. R. *Chem. Vapor Depos.* **2009**, *15*, 39−46.
(28) Wrobel, A. M.; Blaszczyk, I.; Walkiewicz-Pietrzykowska, A.; Tracz, A.; Klembrg-Sapieha, J. E.; Aoki, T.; Hatanaka, Y. *J. Mater. Chem.* **2003**, *13*, 731−737.
(29) Amassian, A.; Vernhes, R.; Klemberg-Sapieha, J. E.; Desjardins, P.; Martinu, L. *Thin Solid Films* **2004**, *469*, 47−53.
(30) Limmanee, A.; Otsubo, M.; Sato, T.; Miyajima, S.; Yamada, A.; Konagai, M. *Jpn. J. Appl. Phys. 1* **2007**, *46*, 56−59.
(31) Huang, H.; Winchester, K. J.; Suvorova, A.; Lawn, B. R.; Liu, Y.; Hu, X. Z.; Dell, J. M.; Faraone, L. *Mater. Sci. Eng. A* **2006**, *435*, 453−459.
(32) Haynes, W. M.; Lide, D. R. *CRC Handbook of Chemistry and Physics: A Ready-Reference Book of Chemical and Physical Data*; Taylor & Francis Group, 2010.
(33) Casserly, T. B.; Gleason, K. K. *Chem. Vapor Depos.* **2006**, *12*, 59−66.
(34) Ohring, M., *Materials Science of Thin Films*; Elsevier Science: Amsterdam, 2001.
(35) Sun, J. W.; Zhang, Y. F.; He, D. Y. *Diam. Relat. Mater.* **2000**, *9*, 1668−1672.
(36) Fainer, N. I.; Rumyantsev, Y. M.; Kosinova, M. L.; Yurjev, G. S.; Maximovskii, E. A.; Kuznetsov, F. A. *Appl. Surf. Sci.* **1997**, *113−114*, 614−617.
(37) Stelzner, T.; Arold, M.; Falk, F.; Stafast, H.; Probst, D.; Hoche, H. *Surf. Coat. Technol.* **2005**, *200*, 372−376.